

# Evaluation of modulus deformation and drainage condition during Cone Loading Tests

A. Teyssier

Fondasol, Avignon, France, [alexandre.teyssier@fondasol.fr](mailto:alexandre.teyssier@fondasol.fr)

P. Reiffsteck

Univ. Gustave Eiffel, IFSTTAR, Marne-la-Vallée, France, [philippe.reiffsteck@ifsttar.fr](mailto:philippe.reiffsteck@ifsttar.fr)

M. Rispal<sup>1</sup>, C. Jacquard<sup>2</sup>,

Fondasol, Avignon, France, [michel.rispal@fondasol.fr](mailto:michel.rispal@fondasol.fr)<sup>1</sup>, [catherine.jacquard@fondasol.fr](mailto:catherine.jacquard@fondasol.fr)<sup>2</sup>

**ABSTRACT:** The static loading of a piezocone by applying incremental steps is one of the only field tests leading to a measure of compression of soil under the cone, shear stress on the shaft and pore pressure between these two points. These three load-deformations curves give valuable information usually impossible to achieve with another ground investigation technique. Herein, the derivation of deformation modulus by cone loading tests (CLT) will be more deeply investigated. The characteristics of the measuring device are detailed, and the accuracy of the deformation measurements is discussed. This paper will present the drainage conditions observed during a cone loading test. Two detailed campaigns, the first performed on a sandy site and the second on a clayey site in southern France are compared to pressuremeter tests (PMT) and to correlations from cone penetration tests (CPT).

**Keywords:** CPTu, cone loading tests, rigidity, pore pressure, drainage condition.

## 1. Introduction

Commonly used ground investigation methods allow the geotechnical engineer to access an important quantity of parameters to characterize soils. These methods, referenced in the ISO/CEN or ASTM standards and the current calculation procedures, permit the building of a geotechnical model, a key element for the geotechnical engineer to design structures.

For this, every ground investigation method brings a set of resistance and/or deformation parameters for soils. However, because of the ground variability or because of budgetary constraints that limit the quantity of tests, these parameters are not directly measured in situ and thus some are deduced by empirical correlations, which have limited validity.

The Cone Penetration Test with porewater pressures, or piezocone (CPTu) is a test used internationally (EN ISO 22476-1). It is highly documented and known as a reliable method to determine mechanical characteristics of soils. This test is mostly executed with fine-grained soils as well as coarse soils with a maximal dimension equal to 20 mm. It allows the determination of the static cone resistance ( $q_c$  or  $q_t$  the total cone resistance with piezocone), the sleeve friction ( $f_s$ ), and the pore pressure ( $u_2$ ). This test gives access to soils resistance, to an estimation of their liquefaction potential, and to an estimation of their permeability. With correlations proposed by Robertson [9], it is also possible to access to their lithological nature, although it is a “blind” test since the soils are not seen but inferred by CPT measurements.

The missing parameter to this method, as to all other cone penetration methods, is the soils deformation parameter which is essential for estimating magnitudes of settlements under a new structure and to consider their

impact on them. It is in this aim that the Cone Loading Test (CLT) has been developed [7], a hybrid test combining the classical probing with the penetrometer and an incremental loading of the cone in order to obtain resistance and deformability parameters.

The test consists in the interruption of the penetration at a chosen depth, followed by the application of axial loads on the cone in successive steps until a failure of the soil beneath is observed. Once the yield point is reached, an unloading with successive steps is performed, allowing to draw a loading/unloading curve linking applied pressures with deformations generated under the cone Fig. 1 et Fig. 2.

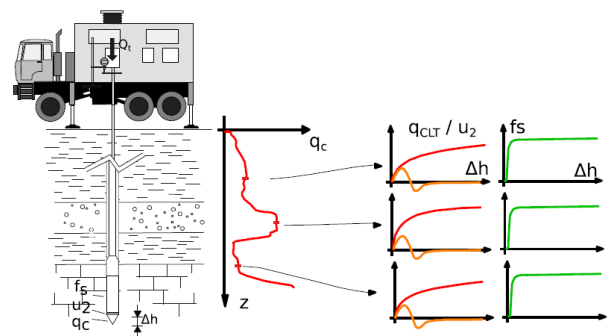


**Figure 1.** Cone Loading Test principles (Reiffsteck., 2017 [2])

The limit cone resistance from the CLT is denoted  $q_{CLT}$ . This is the maximum loading reached at the yield point during the CLT test. It is characterized graphically with a horizontal asymptote. This load is generally smaller than the classical cone resistance ( $q_c$ ) because it is obtained with a quasi-zero speed.

Correspondingly, the limit sleeve friction is noted  $f_{s,CLT}$ . This is the maximum value measured during the cone loading test.

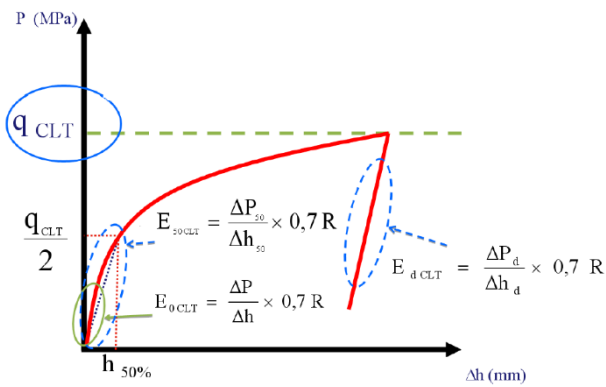


**Figure 2.** Determination of deformation modulus  $E_{0:CLT}$ ,  $E_{50:CLT}$  and  $E_{d:CLT}$  according to the pressure versus deformation curve (after Ali., 2011 [1])

With this curve, three values of deformation moduli are calculated:

- $E_{0:CLT}$ : the initial tangent modulus, estimated with the slope of the first linear part of the loading curve.
- $E_{50:CLT}$ : the modulus at 50% loading, calculated with  $P_{50}$  which is the half of the limit cone resistance ( $q_{CLT}$ ) and with  $\epsilon_{50}$  the associated deformation.
- $E_{d:CLT}$ : the unloading modulus, estimated from the slope of the unloading curve.

Every modulus is weighted by a coefficient of 0.7, where  $R$  is the conical radius and 0.7 is a coefficient considering the conic driving, its geometry, and the soil reshuffle.

A first application to this test is to determine the assessment of an axial pile under a vertical loading using the transformation of the cone resistance curve and the sleeve friction curve to obtain a predictive curve of the assessment depending on the loading [8].

In this paper, after a presentation of the equipment used, the study will provide a comparison between the derived modulus calculated with the loading/unloading curve with CLT and the modulus obtained with traditional investigating methods (i.e., pressuremeter test), as well as values that are obtained from correlations based on CPT data. The impact of drainage conditions will be characterized especially compared between two experimental sites: a sandy site and a clayed site. Finally, the applicability and general conditions of this test, especially its limitations, will be discussed.

## 2. The Cone Loading Test

### 2.1. The penetrometer



**Figure 3.** The static penetrometer vehicle

The test is performed with a heavy static penetrometer vehicle, shown on Fig. 3, which involves pushing a cone probe into the ground at a constant speed of 2 cm/s. The thrust can reach 200 kN.

The cone penetrometer in Fig. 4, in compliance with the EN ISO 22476-1 standards, has a projected area of 10 cm<sup>2</sup>. It allows independent measurements of the cone resistance ( $q_c$ ), the sleeve friction ( $f_s$ ), the pore pressure ( $u_2$ ) and inclination. These measurements are collected in real time inside the CPT truck by a connecting cable that is threaded inside the push rods.

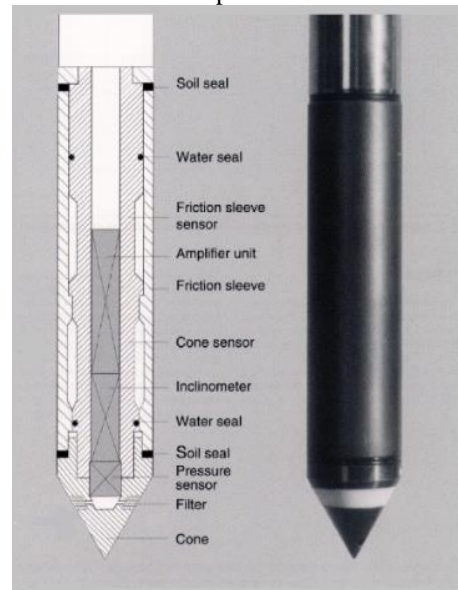


**Figure 4.** The penetrometer cone

The data acquisition system is located at the surface and synchronised in real time to align the cone measurements and those from the depth measurement sensor. A result example from the CPTu is given in Fig. 5.

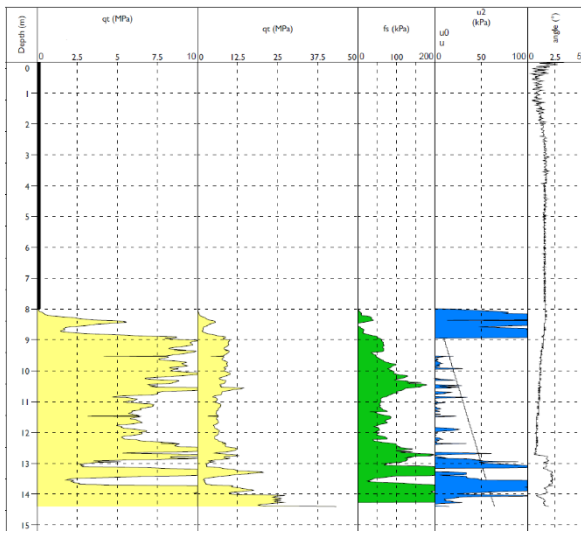


Figure 5. Measurements with a static penetrometer :  $q_c$ ,  $f_s$ ,  $u_2$ , angle

## 2.2. The loading system

The additional thrust device is implemented after the stop of the static penetration at the depth chosen. It consists of a hydraulic cylinder placed between rods and the thrust head of the penetrometer. This jack, controlled by a pressure limiter, is powered by a hydraulic power pack. It allows the application of a controlled thrust on rods independently from the evolution of the soil reaction force.

## 2.3. Instrumentation and measures

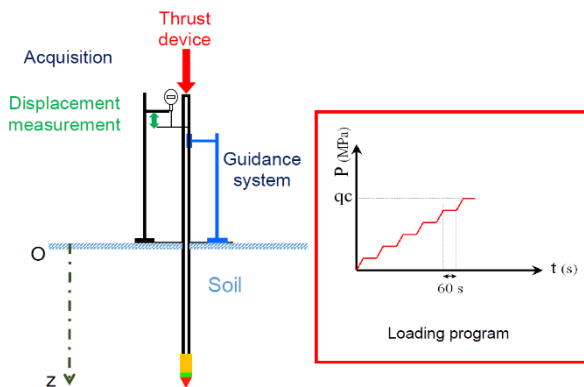


Figure 6. Schematic representation of CLT Test equipment

At the beginning of a CLT test, a dissipation test is launched and recorded by the penetrometer data acquisition system. The acquisition of  $q_c$ ,  $f_s$  and  $u_2$  is then realised continuously, depending on the time. At the same moment, the thrust device at the surface allows the measurement of the pressure in the hydraulic jack, and so the total thrust force on rods corresponding to the  $q_c$  value expected and the displacement of the head of rods. The principle is represented in Fig. 6.

After the application of a corrective factor due to the rods compression, the combination of these two measurements systems will allow the determination of the real displacements of the cone down-hole.

## 2.4. Improvement and prospects

The corrective value due to the rods deformation can be higher than the displacement caused by the soil reaction. The use of a cone penetrometer cone with wireless technologies could allow the measurement directly for more accurate displacement down-hole. It could also free space inside rods for other applications.

## 3. Experimental campaigns

The definition of the scope and the validity of the CLT test needs the realisation of crossed campaigns with traditional investigations (PMT, CPT, laboratory).

Two sites has been chosen for presentation within this paper, as shown on Fig. 7 :

- SETE site with a sandy embankment;
- SARRIANS site with clayed soils.

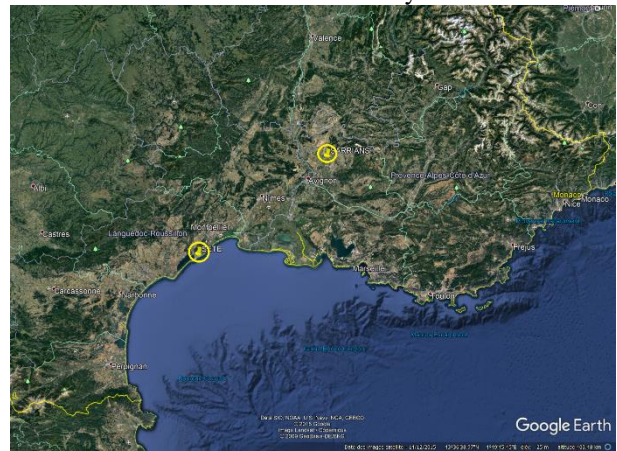


Figure 7. Location of SETE and SARRIANS sites (Google Earth)

## 3.1. Site description and in situ test performed

### 3.1.1. SETE Site (November 2018)

SETE site is a land reclamation built in 2005. It is sensibly flat and horizontal and composed of a sandy embankment on the first 7 meters, then with grey brown sands until 14 meters and finally marly clays.

A vast ground investigation campaign has been realized on this site:

- 3 pressuremeter sounding (PMT) until 20 and 25 m depth.
- 27 cone penetration tests (9 CPT and 18 CPTu), until between 5 and 12.3 m depth.
- 11 geological pits, 2.6 to 2.9 m depth.
- 1 MASW profile, 23 m long.
- Laboratory identifications

Fig. 8 and 9 give a recap of the cone resistance ( $q_c$ ) and the Ménard modulus ( $E_M$ ) characteristics. After a first compact layer on the top (0.5 m), a second sandy layer (6.5 m) is encountered with poor compaction characteristics ( $q_c/q_t < 5$  MPa ;  $E_M < 15$  MPa). Then the mechanical characteristics increase (4 m) in grey brown sands and decrease in marly clays.

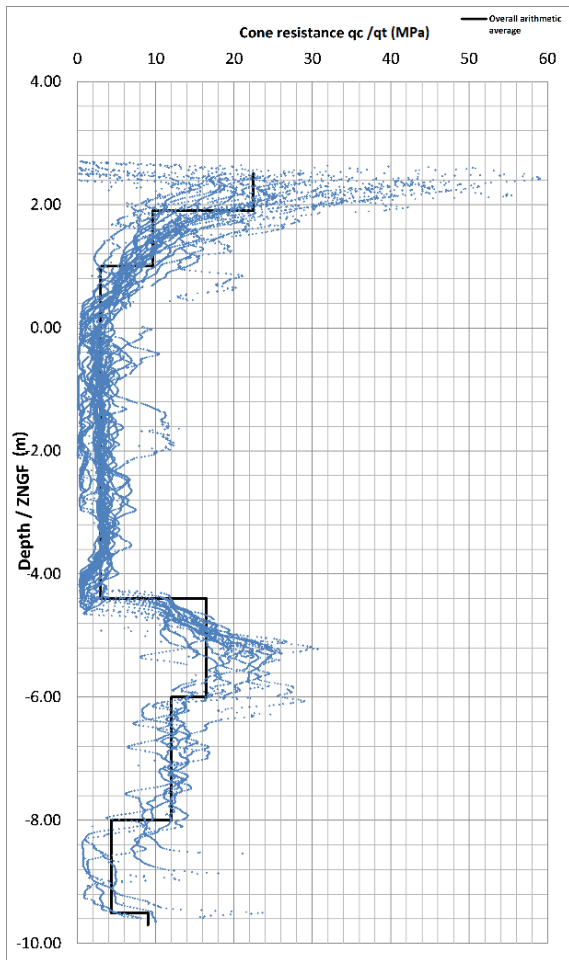


Figure 8. Cone resistance ( $q_c / q_t$ ) measures for SETE site

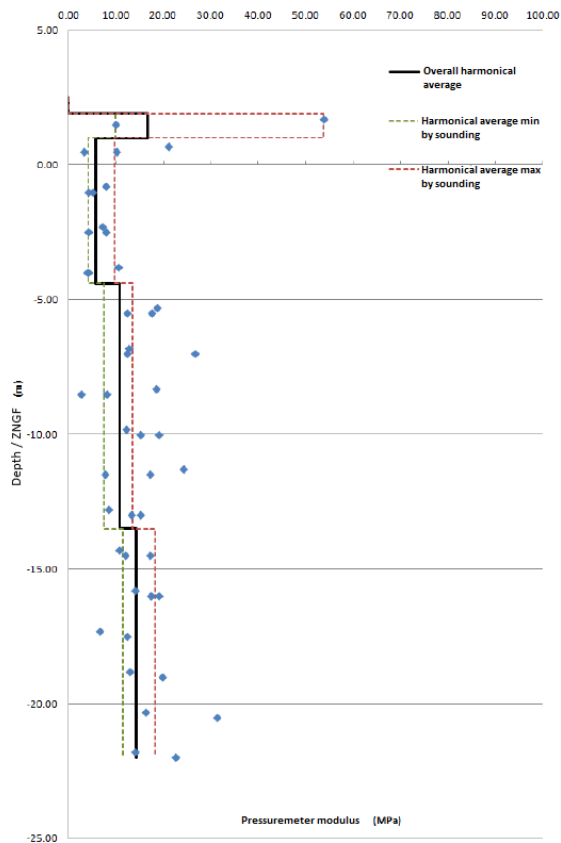


Figure 9. Ménard pressuremeter modulus ( $E_M$ ) measures for SETE site

### 3.1.2. SARRIANS Site (July 2019)

SARRIANS site is flat and horizontal. It is composed of silts and clays until about 10 to 11 meters depths, then encounters with fine grey sands until 13 meters and finally marly clays.

A vast campaign has been done on this site:

- 2 pressuremeter boreholes (PMT) until 10 and 15 m depth.
- 1 core drilling (SC) until 14 m depth.
- 5 electrical cone penetration tests (1 CPT and 4 CPTu), until between 10 and 15.25 m depth.
- 4 geological pits 2.5 to 3.0 m depth.
- Laboratory identifications
- 2 oedometer tests at 6 m and 7 m depth
- 1 triaxial shear test (CU+U) at 1.5 m depth.

Fig. 10 and 11 give a recap of the cone resistance ( $q_c$ ) and the Ménard modulus ( $E_M$ ) characteristics. After a first compact layer on the top (0.5 m), a second clayed layer (11.5 m) is encountered with very poor compaction characteristics ( $q_c/q_t < 2$  MPa ;  $E_M < 10$  MPa). Then the mechanical characteristics increase in the last meters in fine grey sands to marly clays.

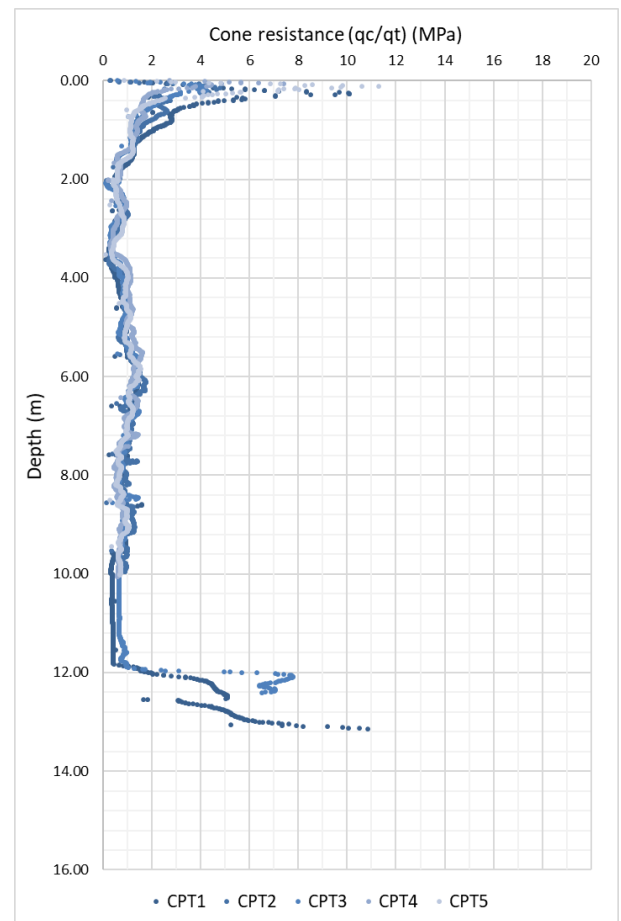


Figure 10. Cone resistance ( $q_c / q_t$ ) measures for SARRIANS site

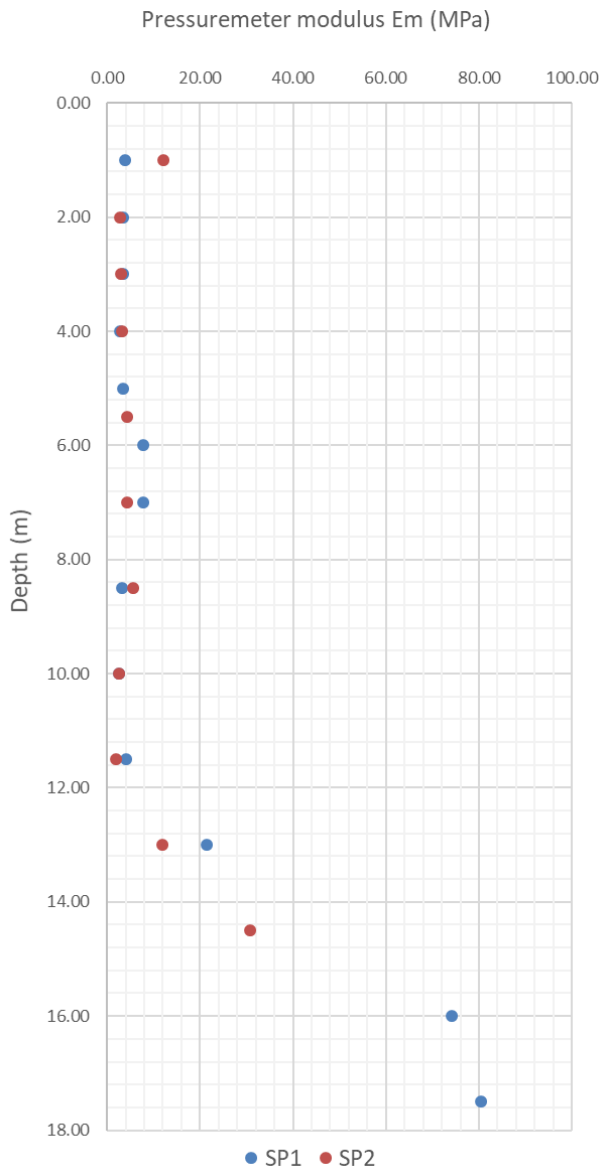


Figure 11. Ménard pressuremeter modulus ( $E_M$ ) measures for SARRIANS site

### 3.2. Laboratory and site test results

Laboratory identification and mechanical tests have been done for SETE and SARRIANS sites, as summarized by Fig. 12 and in Table 1 and Table 2.

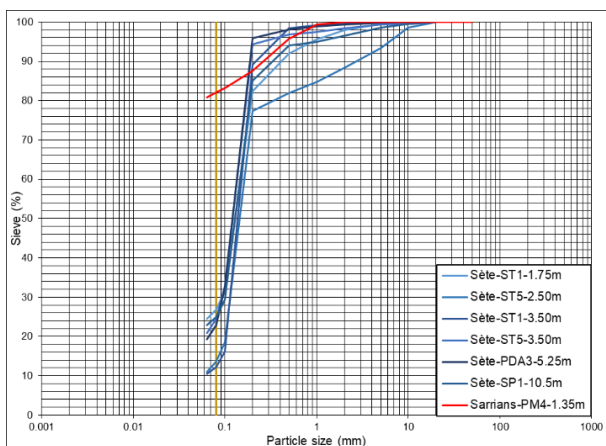


Figure 12. Particle size distributions for SETE and SARRIANS soils

Table 1. Soil classifications for SETE and SARRIANS sites

	$d_{20}$	$d_{30}$	$d_{60}$	NF EN ISO 14688-1
<b>SETE Site :</b>				
ST1-1.75m	-	0.09	0.16	Silty Sand
ST5-2.50m	0.10	0.12	0.17	Sand
ST1-3.50m	0.11	0.12	0.16	Sand
ST5-3.50m	-	0.09	0.14	Silty Sand
PDA3-5.25m	0.07	0.09	0.14	Silty Sand
SP1-10.50m	-	0.1	0.15	Silty Sand
<b>SARRIANS Site :</b>				
PM4-1.35m	-			Clayey Silt

Table 2. Mechanical tests and results for SARRIANS Site

	$C_c$	$C_s$	$e_0$	$c_v$	$\phi'$	$c'$
	-	-	-	$m^2/s$	$^\circ$	$kPa$
SC1-2.25m					26.1	8.1
SC1-6.33m	0.2955	0.0539	0.792	3.6E-8		
SC1-7.37m	0.2965	0.038	0.918	4.4E-7		

An estimation of the permeability based on particle size distribution has been done for the SETE sandy soils, according to the following two formulas:

- Sherard formula Eq. (1) [8], applied for  $0.01 \text{ mm} \leq d_{10} \leq 5 \text{ mm}$

$$k = c_s \left( \frac{d_{15}}{10} \right)^2 \quad (1)$$

With  $0.2 < c_s < 0.6$

- Justin, Hinds & Craeger formula Eq. (2) [1], applied for  $0.005 \text{ mm} \leq d_{10} \leq 2 \text{ mm}$

$$k = \frac{1}{100} 0,342 \cdot d_{20}^{2.294} \quad (2)$$

Permeability results are given in Table 3:

Table 3. Permeability estimation for sandy materials for SETE Site

	Sherard	Justin & al.
ST1-3.50m	3.1E-05 m/s	2.0E-05 m/s
ST5-3.50m	2.6E-05 m/s	1.8E-05 m/s
PDA3-5.25m	-	6.8E-06 m/s

For the clay permeability of SARRIANS site, it has been estimated as being lower than  $1E-06 \text{ m}^2/s$ .

### 3.3. Cone Loading Tests and results

For SETE site, two CLT logs, named CLT2 and CLT3, have been performed close to the pressuremeter borehole SP3.

For SARRIANS site, two CLT logs, named CLT1 and CLT2, have been performed, the first next to the pressuremeter borehole SP2 and the second next to the cone penetration test CPT5.

#### 3.3.1. Example of a CLT test interpretation

A CLT test is performed and interpreted in compliance with the operating procedure defined in Ali's thesis [6]. After a dissipation time of 10 min [6], the cone is pushed in the ground with successive steps, every step being maintained during one minute. Displacements are measured at 15, 30 and 60 sec.

Fig. 13 shows the result of a CLT test.

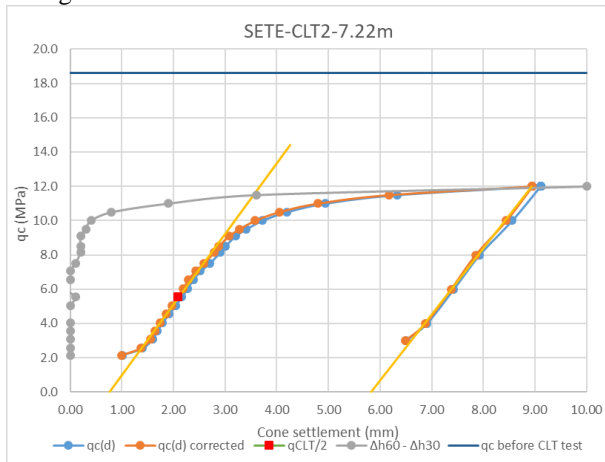


Figure 13. Example of a CLT test interpretation – SETE-CLT2-7.22m

For the CLT at 7.22 m depth, the following modulus are obtained:

- $E_{0CLT} = 52 \text{ MPa}$
- $E_{50CLT} = 34 \text{ MPa}$
- $E_{dCLT} = 49 \text{ MPa}$

The Ménard modulus values obtained in the pressuremeter test SP3 realized nearby, are much lower:

- At 6.5 m,  $E_M = 4 \text{ MPa}$
- At 8 m,  $E_M = 17.5 \text{ MPa}$

Then a comparison will be made between the modulus from CLT tests, Ménard modulus, and modulus calculated from correlations with  $q_c$  from CPT tests.

### 3.3.2. CLT Tests on SETE Site

The eight cone loading tests at the SETE site have been done in layers of sands to silty sands.

Fig. 14, 15 and 16 present the evolution of the cone resistance ( $q_c$ ), the sleeve friction ( $f_s$ ) and the pore pressure ( $u_2$ ) depending of the cone settlement ( $h$ ) during the loading phase of the test, until it reaches the limit cone resistance ( $q_{CLT}$ ), represented with normalised axes.

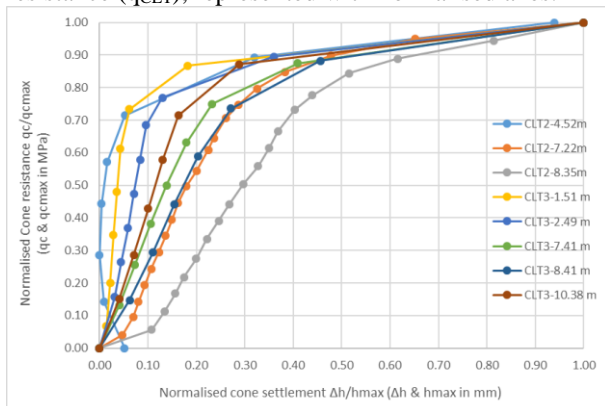


Figure 14. CLT Tests for SETE Site:  $q_c$

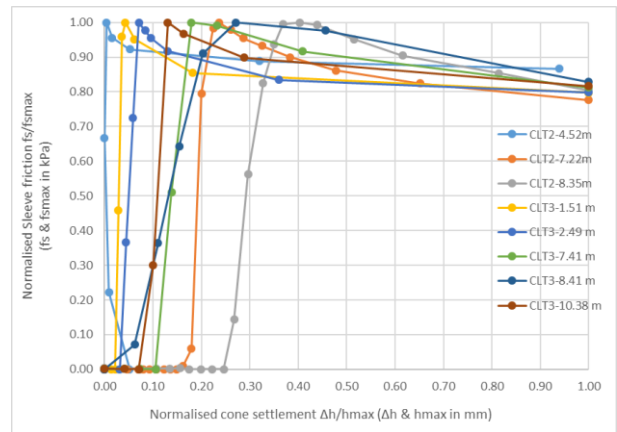


Figure 15. CLT Tests for SETE Site:  $f_s$

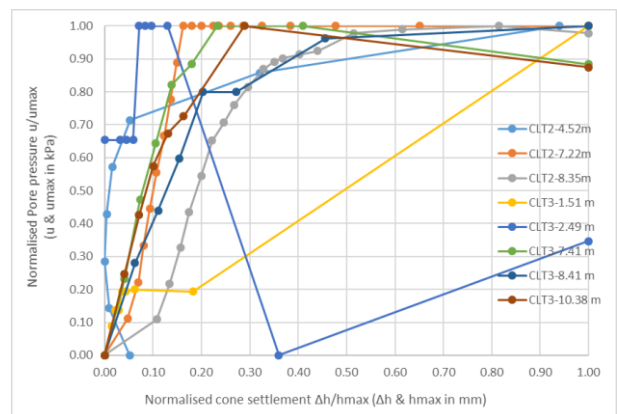


Figure 16. CLT Tests for SETE Site:  $u_2$

The cone resistance ( $q_c$ ) curves between the different tests have the same appearance at the different depths tested. The evolution of the sleeve friction ( $f_s$ ) in sands is characterised by the reach of a peak at a critical deformation and then a relaxation to an asymptote.

The pore pressures ( $u_2$ ) increase rapidly during the test before stabilising. We can note that the tests at 1.51 m and 2.79 m in CLT3 have a different appearance due to the fact that one of these test (1.51 m) has been done out of the groundwater table and the other (2.49 m) at the surface of the groundwater table. In sandy soils, in absolute values, the pore pressure does not vary much because of the quick dissipation allowed by the high permeability of these soils.

### 3.3.3. CLT Tests on SARRIANS Site

All the CLT tests at depths lower than 11 m have been done in clayey silts to silty clays described before. Tests at 11.5 m, 12.5 m and 13 m have been done in a sandy layer.

Fig. 17, 18 and 19 show the evolution of the cone resistance ( $q_c$ ), the sleeve friction ( $f_s$ ) and the pore pressure ( $u_2$ ) depending of the cone settlement ( $h$ ) during the loading phase of the test, until it reaches the limit cone resistance ( $q_{CLT}$ ), represented with normalised axes.

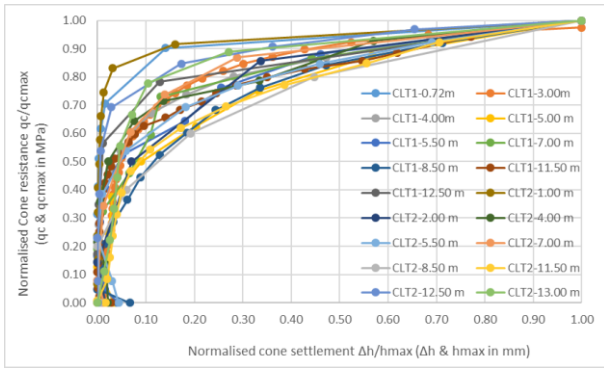


Figure 17. CLT Tests for SARRIANS Site:  $q_c$

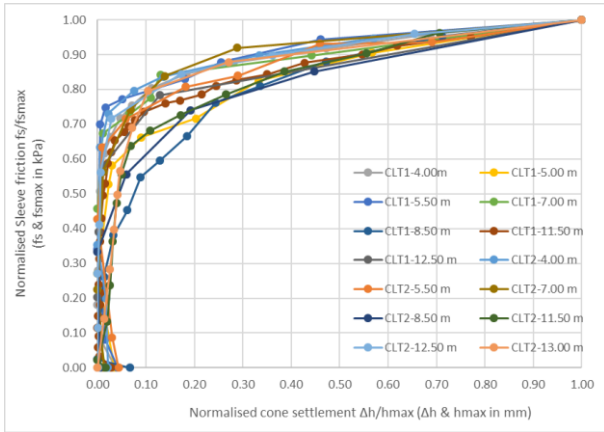


Figure 18. CLT Tests for SARRIANS Site:  $f_s$

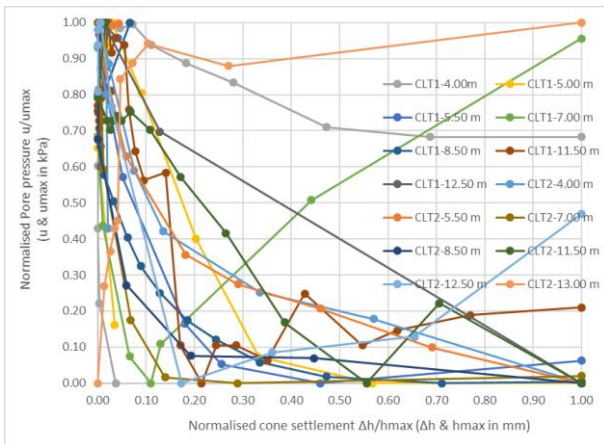


Figure 19. CLT Tests for SARRIANS Site:  $u_2$

The curves of cone resistance ( $q_c$ ) between the different tests have the same appearance at the different depths tested. The sleeve friction ( $f_s$ ) in clays evolves the same as the cone resistance, a progressive increase during the loading phase until it reaches a maximum value at  $q_{CLT}$ .

The pore pressure ( $u_2$ ) has a decreasing tendency during the loading phase of the tests in clays. It increases in one test done in the sandy layer.

## 4. Discussion

### 4.1. CLT Modulus Comparison

Modulus  $E_{0CLT}$ ,  $E_{50CLT}$  et  $E_{dCLT}$  have been derived from the loading / unloading curves of the different CLT. These modulus values are compared to Ménard modulus values ( $E_M$ ) from the closest borehole, to the

$E_M/\alpha$  ratio which is supposed to be close to Young modulus (where  $\alpha$  is the rheological coefficient of Ménéard defined by the type of soil and the  $E_M/p_{LM}$  ratio, and  $p_{LM}$  is Ménéard limit pressure), and finally to the Young modulus obtained by a correlation on the cone resistance ( $q_c$ ) according to Van Impe formulas (1986) Eq. (3) & Eq. (4):

$$E = 3q_c \text{ for } q_c < 5 \text{ MPa} \quad (3)$$

$$E = 7,5 + 1,5q_c \text{ for } 5 < q_c < 30 \text{ MPa} \quad (4)$$

For SETE site, the results are given in Fig. 20 and 21.

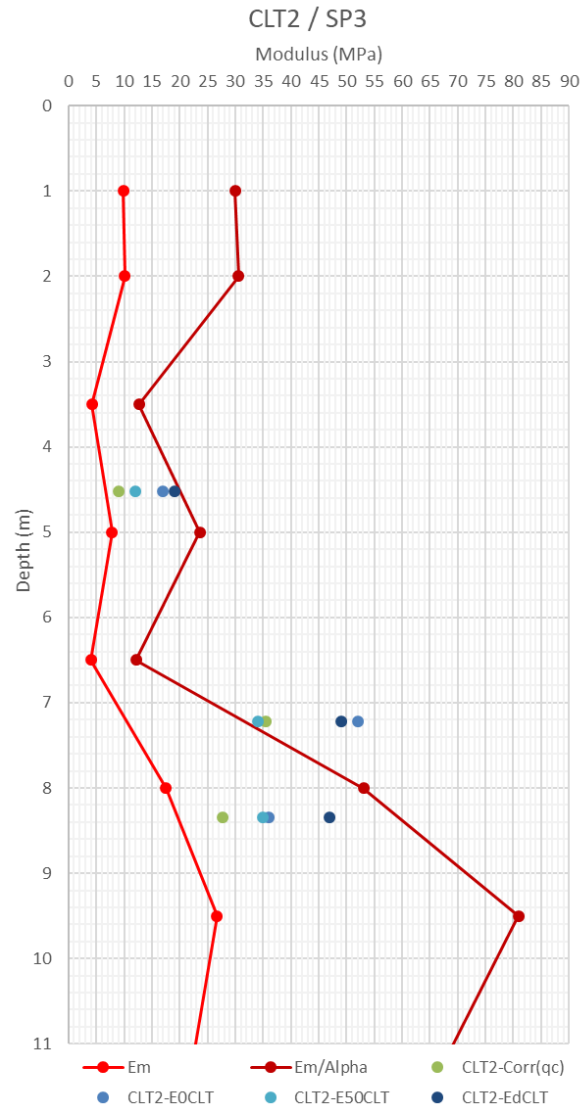
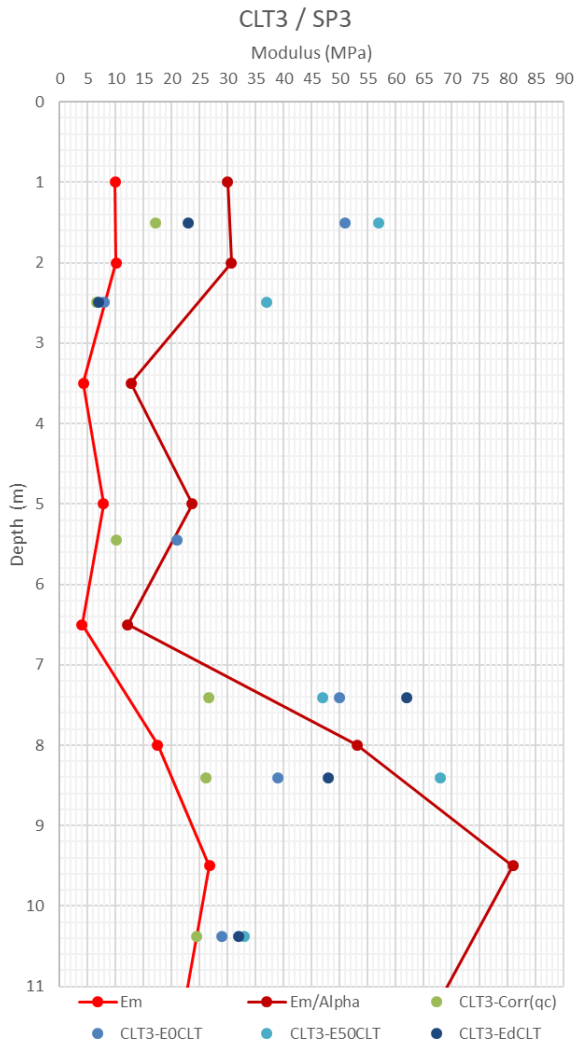


Figure 20.  $E_{0CLT}$  comparison with  $E_M$ ,  $E_M/\alpha$  and Young modulus obtained by CPT correlation, for SETE site (CLT2)



**Figure 21.**  $E_{0CLT}$  comparison with  $E_M$ ,  $E_M/\alpha$  and Young modulus obtained by CPT correlation, for SETE site (CLT3)

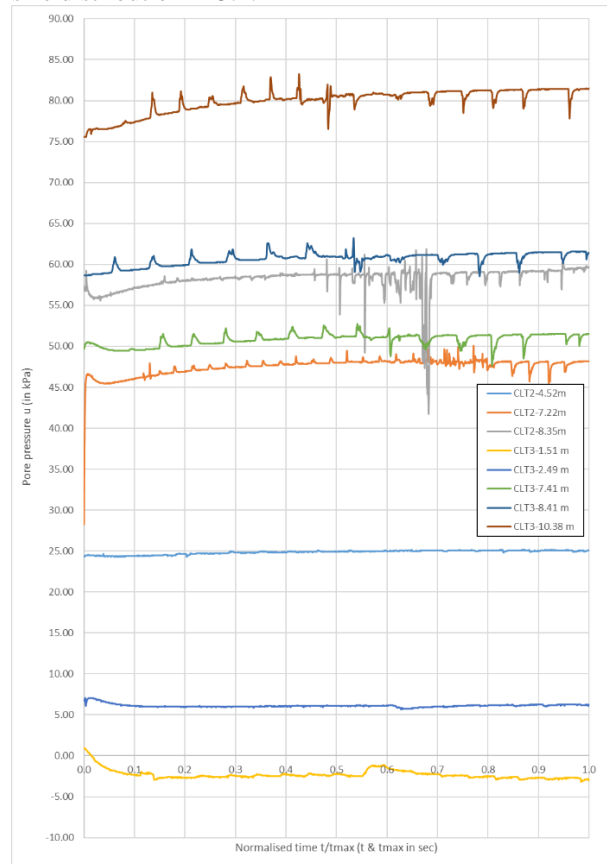
$E_{0CLT}$ ,  $E_{50CLT}$  and  $E_{dCLT}$  modulus obtained have the same order of magnitude than modulus obtained with the ratio  $E_M/\alpha$ . They all are upper than  $E_M$  modulus, which could invite to consider them as equivalent to Young elastic modulus.

For SARRIANS site, displacement values measured in clays at the end of every steps of 60 seconds are too low, despite the application of very small increased pressure, conditioned by the very low consistency of these soils ( $q_c \leq 1$  MPa). The incidence of the corrective coefficient due to the rods elasticity becomes preponderant and does not permit to calculate modulus. We will refer to paragraph 4.3 about the limits of CLT tests.

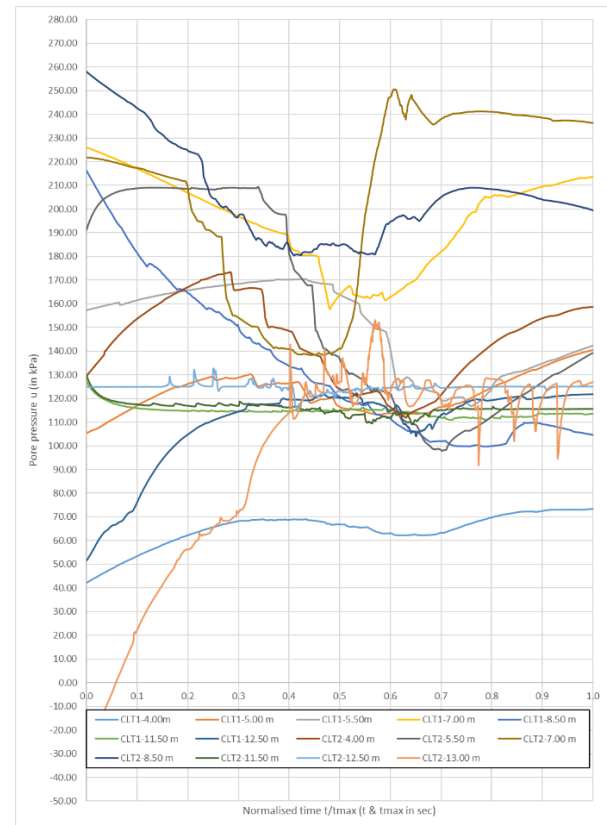
## 4.2. Pore pressure

Fig. 22 and Fig. 23 show the evolution of the pore pressure  $u_2$  during the tests conducted on SETE and SARRIANS sites. For the sandy layers encountered in SETE, drained conditions are observed with almost no variation of the pore pressure from the hydrostatic value. On the SARRIANS site, mixed ground conditions are observed with layers of coarse soils and fine soils. Some curves show almost steady pressures and others present the classical evolution: decrease during the first

loading phase and when failure is reached i.e. close to  $q_{cmax}$ , increase until end of test. These conclusions are in accordance with the permeability derived from particle size distribution in 3.2.



**Figure 22.** Pore pressure  $u_2$  (kPa) during CLT Tests in SETE Site



**Figure 23.** Pore pressure  $u_2$  (kPa) during CLT in SARRIANS Site

### 4.3. Cone Loading Test limits

The realisation of two CLT campaigns, one on a sandy site with a good compactness (SETE) and the other on a clayey site with a very low consistency (SARRIANS) allow a discussion to highlight a few limitations to Cone Loading Tests.

During the test, the displacement is measured according to the pressure applied at the head of rods. Thus to obtain the real displacement of the cone, an estimation of the compression of rods has to be subtracted to the measurement Eq. (5) [7]:

$$h_c = h_m - z \left( \frac{Q_t(h_m) + Q_c(h_m)}{2\pi E_s R^2} \right) \quad (5)$$

It is calculated with the average effort applied on the rods, supposed linearly distributed, between the cone effort and the total effort at the top (z: depth of the test).

For SETE site, with the example of the CLT2 test at 7.22 m, the incidence of the rods correction is presented in Table 4:

**Table 4.** Influence of elastic shortening on conic settlement for SETE Site, CLT2-7.22 m

q <sub>c</sub> (MPa)	h <sub>m</sub> (mm)	Correction (mm)	Correction/h <sub>m</sub> (%)
2.2	1.01	0.011	1.1%
2.6	1.40	0.026	1.9%
3.1	1.59	0.035	2.2%
3.6	1.68	0.044	2.6%
4.1	1.79	0.051	2.9%
4.6	1.91	0.060	3.1%
5.1	2.04	0.067	3.3%
5.6	2.16	0.075	3.5%
6.0	2.27	0.083	3.7%
6.6	2.38	0.091	3.8%
7.1	2.52	0.096	3.8%
7.5	2.70	0.107	4.0%
8.2	2.90	0.116	4.0%
8.5	3.00	0.122	4.1%
9.1	3.20	0.127	4.0%
9.5	3.41	0.130	3.8%
10.0	3.72	0.136	3.7%
10.5	4.19	0.142	3.4%
11.0	4.94	0.146	2.9%
11.5	6.33	0.153	2.4%
12.0	9.11	0.159	1.7%

The incidence of the elastic shortening of rods on displacement measurements is relatively low, and so even if the test had been done deeper. Displacement values recorded during the loading phase until q<sub>CLT</sub> are enough high.

For SARRIANS site, with the example of the CLT1 test at 8.50 m, the incidence of the rods correction is presented in Table 5.

**Table 5.** Influence of elastic shortening on cone settlement for SARRIANS Site, CLT1-8.50 m

q <sub>c</sub> (MPa)	h <sub>m</sub> (mm)	Correction (mm)	Correction/h <sub>m</sub> (%)
0.35	0.02	0.052	289.0%
0.40	0.03	0.053	161.3%
0.45	0.07	0.053	77.1%
0.50	0.12	0.054	45.3%
0.55	0.17	0.055	32.3%
0.60	0.24	0.055	22.8%
0.65	0.34	0.055	16.2%
0.70	0.45	0.056	12.4%
0.75	0.61	0.056	9.2%
0.80	0.86	0.057	6.6%
0.85	1.29	0.057	4.4%
0.90	1.80	0.052	3.2%

On the first steps of the test, displacement values are too low and the rods correction is preponderant, avoiding the determination of E<sub>0CLT</sub> and E<sub>50CLT</sub> modulus. This correction is also preponderant on the low displacement values measured during the unloading phase of the test.

Arbaoui [1] and Reiffsteck [2] have shown however that in stiff clays these difficulties can be overcome. The friction-limiting tool used in the present research is probably not sufficiently efficient. The shaft friction stay mobilized on the rods and when a load is reached the rapid movement is a major problem. The use of another type of cone (15 cm<sup>2</sup>) may solve this point.

### 5. Conclusions

The Cone Loading Test is a loading / unloading test that can easily be coupled with a static cone penetration test campaign to acquire a soil deformability parameter at different depths.

It allows elasticity moduli to be calculated that are close to Young modulus estimated by the E<sub>M</sub> / α ratio from the Ménard pressuremeter test.

The campaigns of SETE (moderately compact sands) and SARRIANS (very soft clays) involve very different soils and have highlighted a limitation of this test, difficult to apply in certain soils with corresponding displacements, due to the elasticity of the stems, can become predominant.

In perspective, it would be necessary to carry out new campaigns on areas of sufficient density to perform comparative calculations of deformations, for example for the design of foundations, between plate load tests, Ménard pressuremeter direct design method and CLT method.

## 6. Acknowledgement

The project presented in this article is supported by the Industrial Port of SETE and SARRIANS Town Hall, which allow us to access to the different sites for our experimental campaigns.

## 7. References

- [1] Arbaoui H., Gourvès R., Bressolette Ph., Bodé L., "Mesure de la déformabilité des sols in situ à l'aide d'un essai de chargement statique d'une pointe pénétrométrique", (Measurement of soils deformability in situ using a static loading test with a penetrometer cone) *Can. Geotech. J.*, 2006. (in French), 43(4) 355-369.
- [2] Reiffsteck Ph., Bacconnet C., Gourvès R., van de Graaf H.C., Thorel L. "Measurements of soil compressibility by means of cone penetrometer", *Soils and Foundations*, 2009, 49(3) 397-408.
- [3] Reiffsteck P., Bacconnet C., Gourves R., Godde E., Van De Graaf H., "Determination of elastic modulus from stress controlled cone penetration test", 3rd International conference on Site Characterization, 2008, Taipei, pp. 1135-1138.
- [4] Ali H., Reiffsteck Ph., Baguelin F., Van de Graaf H., Bacconnet C., Gourvès R., "Settlement of pile using Cone Loading Test: Load Settlement Curve Approach", *CPT 10*, 2010, Huntington beach Los Angeles.
- [5] Ali H. & Reiffsteck Ph., Thorel L., Gaudin C., "Influence factors study of cone loading test in the centrifuge", *CPT'10*, 2010, Huntington beach, P. Robertson Ed.
- [6] Ali H. "Caractérisation améliorée des sols par l'essai de chargement de pointe au piezocone – Application au calcul des fondations profondes", (Improved characterization of soils by the Cone Loading Test – Application to calculation of deep foundations) Doctoral degree, University Blaise Pascal – Clermont-Ferrand II, 2010. (in French) [online] Available at: <https://tel.archives-ouvertes.fr/tel-00629642> [Accessed: 01/12/2016].
- [7] Khoury N., Zaman M., Ghabchi R., Kazmee H. "Stability and permeability of proposed aggregate bases in Oklahoma", School of Civil Engineering and Environmental Science – The University of Oklahoma, 2010. [online] Available at: [www.okladot.state.ok.us > reports > rad\\_spr2-i2196-fy2009-rpt-final-zaman](http://www.okladot.state.ok.us/reports/rad_spr2-i2196-fy2009-rpt-final-zaman) [Accessed: 13/11/2015].
- [8] Reiffsteck Ph., van de Graaf H., Jacquard C., "Assessment of pile bearing capacity and load-settlement behavior, based on cone loading test (CLT) results", *CPT18, 4th Int Symp. on Cone Penetration Testing*, 2018, Delft.
- [9] Robertson P.K., Interpretation of cone penetration tests — a unified approach, *Can. Geotech.*, 2009, J.46: 1337–1355 doi:10.1139/T09-065